



# Entropy analysis on oscillating flow of third grade nanofluid in a channel with Joule heating: a Buongiorno model approach

K. Govindarajulu<sup>1,a</sup>, A. Subramanyam Reddy<sup>1,b</sup> , Ali J. Chamkha<sup>2,c</sup>

<sup>1</sup> Department of Mathematics, Vellore Institute of Technology, Vellore, Tamil Nadu 632014, India

<sup>2</sup> Faculty of Engineering, Kuwait College of Science and Technology, 35004 Doha, Kuwait

Received: 22 March 2022 / Accepted: 2 May 2023

© The Author(s), under exclusive licence to Società Italiana di Fisica and Springer-Verlag GmbH Germany, part of Springer Nature 2023

**Abstract** In the current investigation, hydromagnetic third grade pulsating nanofluid flow through a channel under the influence of Brownian motion, thermophoresis, radiative heat has been inspected. The influence of viscous dissipation, chemical reaction, and Ohmic heating is considered in the current investigation. The Buongiorno nanofluid model is implemented, and the analysis of entropy generation is carried out. The present investigation may be applicable in the fields of biomedical engineering, manufacturing industries as coolants, pressure surges, energy conservation, and nano-drug suspension in pharmaceuticals. The perturbation technique is employed on flow governing equations (partial differential equations (PDEs)) to convert into a set of ordinary differential equations (ODEs). The shooting process along with the support of Runge–Kutta fourth-order method is employed to solve the set of nonlinear ODEs. The impressions of dimensionless emerging physical parameters on pertinent flow variables are demonstrated by using graphical illustrations. The results portrayed that intensifying the Hartmann number, non-Newtonian, frequency, and material parameters decline the velocity of the nanofluid. Augmenting the Eckert number, Brownian motion, and thermophoresis parameter enhance the temperature whereas accelerating the radiation parameter and Hartmann number reduces the temperature. The nanoparticles concentration is enhanced for a rise in Brownian motion, while it decelerates for the higher values of Lewis number. The entropy and Bejan number are accelerated with the increment in radiation parameter. The heat and mass transfer rates are raised for augmenting the value of Brownian motion parameter.

## 1 Introduction

Nowadays, many researchers and scientists are concentrated on the nanofluid-oriented investigations because of the physical properties and applications of nanofluids in biomedical and manufacturing industries as well as in science and technology. Nanofluids are used for nano-drug delivery, automobile applications, food production, solar energy, photodynamic therapy, space technology, and nuclear reactors [1, 2]. To enhance the heat transfer rate and thermal conductivity of the conventional base fluids such as water, engine oil, Ethylene glycol, blood, and lubricants, the nanosized particles are deployed into base fluids. Choi and Eastman [3] noticed the abnormal development in heat transfer and thermal conductivity when nanoparticles are suspended into traditional base fluids, and these fluids are called as nanofluids. A new nanofluid model was proposed and investigated the Brownian motion and thermophoretic effects by Buongiorno [4]. Shah et al. [5] studied the effects of Brownian motion and thermophoresis on the third grade nanofluid flow through the rotating parallel plates by applying the homotopy analysis technique. Kumar et al. [6] inspected the radiative heat, magnetic field, thermophoretic, and Brownian diffusion effects on pulsatile Casson nanofluid flow in a vertical permeable channel by utilizing Buongiorno nanofluid model. Hayat et al. [7] numerically analyzed the third grade nanofluid flow via nonlinear elastic surface with magnetic field, chemical reaction, activation energy, and Brownian diffusion impacts by using NDSolve in Mathematica. Naz et al. [8] analytically studied the entropy on magnetohydrodynamic (MHD) flow of Carreau nanofluid past a cylinder with Brownian and thermophoretic effects by using optimal homotopy analysis method. Chu et al. [9] examined the effect of chemical reaction with activation energy on hydromagnetic third grade nanofluid flow upon an elastic surface by considering Buongiorno nanofluid model. Derikvand et al. [10] numerically investigated the entropy production and heat transfer of  $H_2O + Al_2O_3$ -based non-Newtonian nanofluid in a permeable medium with flow injection and hydrophobic walls. Khan et al.

K Govindarajulu, A Subramanyam Reddy, and Ali J Chamkha contributed equally to this work.

<sup>a</sup> e-mail: govind047@gmail.com

<sup>b</sup> e-mail: anala.subramanyamreddy@gmail.com (corresponding author)

<sup>c</sup> e-mail: achamkha@yahoo.com

[11] analytically inspected the mass and heat transfer using the theory of Cattaneo–Christov on non-Newtonian nanofluid flow via enlargeable sheet under magnetic field, Brownian and thermophoresis effects by utilizing the homotopy analysis approach.

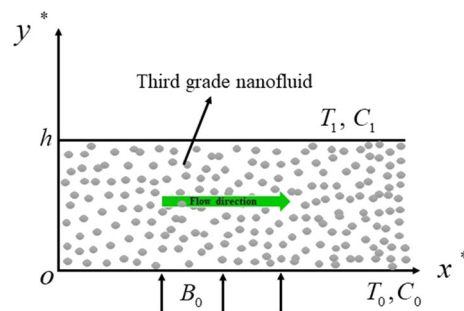
The non-Newtonian fluids have received much attention in the research community due to their applications and rheological characteristics. The major applications of non-Newtonian fluids in the fields of industries, science, and technology such as paper production, wiring coating, food processing, nourishment preparing, crystal growth, cosmetics, coal slurries, clay mixture, oil recovery, rubber, and plastic sheet drawing. Based on the various rheological properties of non-Newtonian fluids, it is difficult to give a unique constitutive relation for non-Newtonian fluids. So, they are classified into three types namely, integral, rate, and differential. The third grade fluid falls into the subclass of differential type that shows both shear thinning and thickening behavior [12–15]. Hussain et al. [16] numerically scrutinized the MHD third grade nanofluid flow over a stretchable sheet with Ohmic heating, solar radiation, thermophoresis, and Brownian motion effects by applying the homotopy analysis method. Abbasi et al. [17] inspected the impacts of thermal radiation, chemical reaction, Brownian and thermophoretic diffusions on third grade nanofluid stagnation point flow past a vertically lubricated surface by applying the Keller box method. Henda et al. [18] analyzed the hydromagnetic bioconvection stagnation dot flow of third grade nanofluid past an expandible cylinder with the effects of radiative heat, Brownian motion, activation energy, and thermophoresis by using Buongiorno model. Xu et al. [19] numerically explored the influence of activation energy, induced magnetic field, Brownian diffusion, and non-uniform heat generation/absorption on third grade nanofluid flow in a stretching plate by applying shooting procedure. Recently, Govindarajulu and Reddy [20] numerically inspected the impacts of viscous dissipation, magnetic field, and thermal radiation on third grade hybrid nanofluid flow in a penetrable channel with pulsatile pressure gradient.

The pulsatile flow concerning investigations in a pipe or channel create a huge intention among scientists and researchers because of its practical applications in the areas of biomedical, industries, and mechanical engineering. For example, respiratory systems, thermal insulation, urine flow in the ureter, the cooling of electronic components, circulatory systems, air conditioning, IC engines, vascular diseases, geothermal systems, reciprocating pumps, and blood dialysis process in an artificial kidneys [21–24]. Shawkly [25] inspected the heat transfer of non-Newtonian dusty nanofluid flow via channel with the impacts of magnetic field and pulsatile pressure gradient by using Lighthill method. Qomi et al. [26] explored the two kinds of heat source on hydromagnetic pulsatile hybrid nanofluid flow through microchannel by using the transient approach. Venkatesan and Reddy [27] analytically scrutinized the pulsatile flow of non-Newtonian nanofluid via permeable channel under magnetic field, dissipative viscous, Ohmic heating, and thermal radiation impacts by utilizing the perturbation procedure. Ahmed and Xu [28] investigated the pulsatile hybrid nanofluid flow through microchannel with the effects of magnetic field and radiative heat by employing the perturbation method. Kardgar [29] numerically inspected the non-Newtonian oscillating nanofluid flow through a cavity under the external magnetic field by employing the finite volume method. Here, the authors analyzed their study without considering the viscous dissipation and Ohmic heating impacts. Rajkumar and Reddy [30] explored the influence of applied magnetic field, Ohmic heating, radiative heat, and viscous dissipation on electrically induced pulsatory non-Newtonian nanofluid flow through permeable channel by applying the Runge–Kutta forth-order procedure. Esfe et al. [31] made a critical review to explore the thermal and hydraulic properties of pulsatory flow of classical heat transfer liquids and inventive nanofluids. Venkatesan and Reddy [32] analytically inspected the magnetohydrodynamic pulsatile non-Newtonian nanofluid flow via channel in the presence of thermal radiation, viscous dissipation, and Ohmic heating by employing the perturbation procedure.

The purpose of introducing entropy production is to estimate the amount of irreversible and unavailable energies in the system. This kind of analysis helps to accelerate the thermal efficiency and creates a necessity to utilize the energy. The entropy generation plays a significant role in nuclear reactors, coolers, power plants, heat engines and pumps, air chillers, and solar energy systems [33–36]. Hayat et al. [37] scrutinized the entropy production on MHD third grade nanofluid flow through a permeable stretching surface with chemical reaction, thermophoresis, and Brownian diffusion impacts. Loganathan et al. [38] analyzed the entropy optimization on third grade nanofluid flow past a stretchy sheet in the presence of magnetic field, thermal radiation, and Brownian motion effects. Khan et al. [39] numerically studied the impacts of chemically reactive species, magnetic field, and Darcy Forchheimer on non-Newtonian nanofluid flow over a nonlinear expandable sheet with entropy production by utilizing the Runge–Kutta fifth-order scheme. Li et al. [40] numerically explored the Marangoni solutal convective Casson hybrid nanofluid flow past a disk under entropy production with radiative heat, nonlinear heat source/sink, and viscous dissipation effects by employing bvp4c in MATLAB. Ahmad et al. [41] inspected the stagnation point flow of micropolar nanofluid over an elastic nonlinear surface under partial slip, buoyancy effect, and entropy with Cattaneo–Christov heat flux model by applying the finite difference scheme along with bvp4c from MATLAB.

The main objective of the current investigation is to inspect the MHD pulsatile flow of third grade nanofluid with the impacts of viscous dissipation, Joule heating, thermophoresis, radiative heat, and Brownian motion in a channel. The aforementioned literature survey reveals that there has been no study concerning this kind of investigation yet. The Buongiorno nanofluid model is implemented with entropy production in the present study. The impacts of chemical reaction, Joule heating, Brownian diffusion, thermophoresis, and heat source/sink on MHD pulsating third grade nanofluid through a channel with entropy generation by applying Buongiorno model is the main novelty of the current analysis. This investigation is noteworthy in many fields such as solar energy, dynamics of physiological fluids, space technology, defence and military, biomedicine, and cancer therapeutic as well as in industrial processes. The flow governing PDEs are transmitted to a set of ODEs through the perturbation approach, then numerically solved by implementing shooting procedure together with the Runge–Kutta fourth-order procedure. The impacts of numerous

**Fig. 1** Physical sketch of the problem



pertinent physical parameters on velocity, concentration, and temperature are described graphically. Owing to the importance of this kind of problem, the present analysis aims to manifest answers to the following research questions:

- (i) What are the impacts of frequency parameter and Hartmann number on velocity distribution of nanofluid?
- (ii) How do the temperature distribution profile of nanofluid influenced by the Brownian motion, thermophoresis diffusion, thermal radiation, and heat source/sink?
- (iii) What are the impact of chemical reaction and Lewis number on concentration distribution profile of third grade blood-based nanofluid?
- (iv) What is the importance of analyzing entropy generation rate and Bejan number?
- (v) What is the significance of magnetic field, thermophoresis, and Brownian motion on heat and mass transfer rate of third grade nanofluid?

## 2 Formation of the problem

We consider an electrically conducting incompressible, laminar, hydromagnetic pulsating flow of third grade nanofluid through horizontal parallel plates with Joule heating, Brownian motion, and thermophoresis effects. The influence of viscous dissipation, thermal radiation, and chemical reaction rate is considered into the account. As presented in Fig. 1, a coordinate system is chosen as follows: The  $x^*$ -axis is along with the bottom wall of the channel, and the  $y^*$ -axis is orthogonal to the walls, and  $h$  is the distance between the walls. A magnetic field of strength  $B_0$  is uniformly applied orthogonal to the flow direction. The top and bottom walls of the channel maintain the constant temperatures  $T_1, T_0$  ( $T_1 > T_0$ ) and concentrations  $C_1, C_0$  ( $C_1 > C_0$ ), respectively. The constitutive equation for third grade fluid model is [14, 15].

$$S_i = -pI + \mu B_1^* + \alpha_1 B_2^* + \alpha_2 B_1^{*2} + \beta_1 B_3^* + \beta_2 (B_1^* B_2^* + B_2^* B_1^*) + \beta_3 (tr B_1^{*2}) B_1^*, \tag{1}$$

here,  $p$  is the pressure,  $I$  is the identity tensor,  $\mu$  is dynamic viscosity, and  $\alpha_1, \alpha_2, \beta_1, \beta_2,$  and  $\beta_3$  are material constants.  $B_1^*, B_2^*,$  and  $B_3^*$  are the first three Rivlin–Ericksen (kinematic) tensors and are defined as follows:

for  $n = 1, 2, 3, \dots$

$$B_n^* = \frac{dB_{n-1}^*}{dt} + B_{n-1}^* (\text{grad}V) + (\text{grad}V)^t B_{n-1}^*. \tag{2}$$

Here,  $B_0^* = I, V$  is velocity field and  $\frac{d}{dt}$  is material time derivative. Now, considering Eq. (1) is compatible with the thermodynamics, and the following constraints are employed,

$$\mu \geq 0, \alpha_1 \geq 0, \beta_1 = \beta_2 = 0, \beta_3 \geq 0, \text{ and } |\alpha_1 + \alpha_2| \leq \sqrt{24\mu\beta_3}. \tag{3}$$

Now, using Eq. (3), Eq. (1) becomes

$$S_i = -pI + \mu B_1^* + \alpha_1 B_2^* + \alpha_2 B_1^{*2} + \beta_3 (tr B_1^{*2}) B_1^*. \tag{4}$$

With these concerned considerations, we derived the flow governing equations as

$$\rho_f \frac{\partial u^*}{\partial t^*} = -\frac{\partial P^*}{\partial x^*} + \mu_f \frac{\partial^2 u^*}{\partial y^{*2}} + \alpha_1 \left( \frac{\partial^3 u^*}{\partial t^* \partial y^{*2}} \right) + 6\beta_3 \left( \frac{\partial u^*}{\partial y^*} \right)^2 \left( \frac{\partial^2 u^*}{\partial y^{*2}} \right) - \sigma_f B_0^2 u^*, \tag{5}$$

$$\frac{\partial T^*}{\partial t^*} = \frac{k_f}{(\rho C_p)_f} \frac{\partial^2 T^*}{\partial y^{*2}} + \frac{\sigma_f}{(\rho C_p)_f} B_0^2 u^{*2} + \frac{\mu_f}{(\rho C_p)_f} \left( \frac{\partial u^*}{\partial y^*} \right)^2 + 2 \frac{\beta_3}{(\rho C_p)_f} \left( \frac{\partial u^*}{\partial y^*} \right)^4 - \frac{1}{(\rho C_p)_f} \frac{\partial q_r}{\partial y^*} + \tau \left[ D_B \frac{\partial C^*}{\partial y^*} \frac{\partial T^*}{\partial y^*} + \frac{D_T}{T_m} \left( \frac{\partial T^*}{\partial y^*} \right)^2 \right] + Q_0 (T^* - T_0), \tag{6}$$

$$\frac{\partial C^*}{\partial t^*} = D_B \frac{\partial^2 C^*}{\partial y^{*2}} + \frac{D_T}{T_m} \frac{\partial^2 T^*}{\partial y^{*2}} - k_1 C^*. \tag{7}$$

Here,  $u^*$  is the velocity component in the  $x^*$ - direction,  $P^*$  is the fluid pressure,  $\rho_f$  is density of the fluid,  $\mu_f$  is the viscosity of fluid,  $\alpha_1, \beta_3$  are material constants,  $\sigma_f$  is electrical conductivity of the fluid,  $k_f$  is thermal conductivity, and  $(\rho C_p)_f$  is effective specific heat of the fluid.  $T^*$  is the temperature,  $C^*$  is the concentration of nanoparticles,  $q_r$  is the radiative heat flux,  $\tau = \frac{(\rho C_p)_p}{(\rho C_p)_f}$ ,  $(\rho C_p)_p$  is the effective heat capacity of the nanoparticles,  $Q_0$  is heat source/sink coefficient,  $D_B$  and  $D_T$  are Brownian diffusion and thermophoretic diffusion coefficients, respectively,  $T_m$  is mean temperature, and  $k_1$  is the first order chemical reaction.

The corresponding boundary conditions (B.Cs) are

$$\text{at } y^* = 0 \Rightarrow u^* = 0, T^* = T_0, C^* = C_0, \tag{8}$$

$$\text{at } y^* = h \Rightarrow u^* = 0, T^* = T_1, C^* = C_1. \tag{9}$$

By applying the Rosseland approximation for radiative heat flux ( $q_r$ ), Eq. (6) becomes

$$\begin{aligned} \frac{\partial T^*}{\partial t^*} = & \frac{k_f}{(\rho C_p)_f} \frac{\partial^2 T^*}{\partial y^{*2}} + \frac{\sigma_f}{(\rho C_p)_f} B_0^2 u^{*2} + \frac{\mu_f}{(\rho C_p)_f} \left( \frac{\partial u^*}{\partial y^*} \right)^2 + 2 \frac{\beta_3}{(\rho C_p)_f} \left( \frac{\partial u^*}{\partial y^*} \right)^4 \\ & + \frac{1}{(\rho C_p)_f} \left( \frac{16\sigma^* T_1^3}{3\kappa^*} \right) \frac{\partial^2 T^*}{\partial y^{*2}} + \tau \left[ D_B \frac{\partial C^*}{\partial y^*} \frac{\partial T^*}{\partial y^*} + \frac{D_T}{T_m} \left( \frac{\partial T^*}{\partial y^*} \right)^2 \right] \\ & + Q_0(T^* - T_0), \end{aligned} \tag{10}$$

here,  $\kappa^*$  is Rosseland mean absorption coefficient, and  $\sigma^*$  is Stefan–Boltzmann constant.

Now, the dimensionless parameters and variables are chosen as follows:

$$u = \frac{u^*}{U}, x = \frac{x^*}{h}, y = \frac{y^*}{h}, t = t^* \omega, P = \frac{hP^*}{\mu_f U}, \theta = \frac{T^* - T_0}{T_1 - T_0}, \phi = \frac{C^* - C_0}{C_1 - C_0}. \tag{11}$$

By utilizing Eq. (11), Eqs. (5), (7), and (10) are converted to:

$$\frac{\partial u}{\partial t} = -\frac{1}{H^2} \frac{\partial P}{\partial x} + \frac{1}{H^2} \frac{\partial^2 u}{\partial y^2} + \frac{1}{H^2} \gamma \frac{\partial^3 u}{\partial t \partial y^2} + \frac{6}{H^2} \Delta_1 \left( \frac{\partial u}{\partial y} \right)^2 \left( \frac{\partial^2 u}{\partial y^2} \right) - \frac{1}{H^2} M^2 u, \tag{12}$$

$$\begin{aligned} \frac{\partial \theta}{\partial t} = & \left( 1 + \frac{4Rd}{3} \right) \frac{1}{H^2 Pr} \frac{\partial^2 \theta}{\partial y^2} + \frac{Ec}{H^2} M^2 u^2 + \frac{Ec}{H^2} \left( \frac{\partial u}{\partial y} \right)^2 + 2 \frac{Ec}{H^2} \Delta_1 \left( \frac{\partial u}{\partial y} \right)^4 \\ & + \frac{Q}{H^2} \theta + \frac{Nb}{H^2} \frac{\partial \phi}{\partial y} \frac{\partial \theta}{\partial y} + \frac{Nt}{H^2} \left( \frac{\partial \theta}{\partial y} \right)^2, \end{aligned} \tag{13}$$

$$\frac{\partial \phi}{\partial t} = \frac{1}{H^2 Pr Le} \frac{\partial^2 \phi}{\partial y^2} + \frac{1}{H^2 Pr Le} \frac{Nt}{Nb} \frac{\partial^2 \theta}{\partial y^2} - \frac{\gamma_1}{H^2} \phi - \frac{K_1}{H^2}, \tag{14}$$

here,  $H = \sqrt{\frac{\omega h^2}{\nu_f}}$  is frequency parameter,  $U$  is characteristic velocity,  $\Delta_1 = \frac{\beta_3 U^2}{\mu_f h^2}$  is non-Newtonian coefficient,  $\gamma = \frac{\alpha_1 \omega}{\mu_f}$  is the material parameter for third grade fluid,  $Pr = \frac{(\rho C_p)_f \nu_f}{k_f}$  is Prandtl number,  $M = B_0 h \sqrt{\frac{\sigma_f}{\mu_f}}$  is Hartmann number,  $Rd = \frac{4\sigma^* T_1^3}{\kappa^* k_f}$  is the radiation parameter,  $Ec = \frac{U^2}{(C_p)_f (T_1 - T_0)}$  is the Eckert number,  $Nb = \frac{\tau D_B (C_1 - C_0)}{\nu_f}$  is Brownian motion parameter,  $Nt = \frac{\tau D_T (T_1 - T_0)}{T_m \nu_f}$  is thermophoresis parameter,  $Q = \frac{Q_0 h^2}{(\rho C_p)_f \nu_f}$  is heat sink/source parameter,  $Le = \frac{k_f}{D_B (\rho C_p)_f}$  is Lewis number,  $\gamma_1 = \frac{k_1 h^2}{\nu_f}$  is chemical reaction parameter,  $K_1 = \frac{k_1 C_0 h^2}{\nu_f (C_1 - C_0)}$  is constant, and  $\omega$  is frequency.

The appropriate BCs are

$$\text{at } y = 0 \Rightarrow u = 0, \theta = 0, \phi = 0, \tag{15}$$

$$\text{at } y = 1 \Rightarrow u = 0, \theta = 1, \phi = 1. \tag{16}$$

### 3 Solution of the problem

Since the flow is induced by the pressure gradient, the dimensionless pressure gradient is taken as follows:

$$-\frac{\partial P}{\partial x} = \lambda_0 + \varepsilon \lambda_1 e^{it}. \tag{17}$$

On basis of Eq. (17), the solutions for  $u, \theta,$  and  $\phi$  are expressed as follows:

$$u = u_0 + \varepsilon u_1 e^{it}, \tag{18}$$

$$\theta = \theta_0 + \varepsilon \theta_1 e^{it}, \tag{19}$$

$$\phi = \phi_0 + \varepsilon \phi_1 e^{it}. \tag{20}$$

Now, taking Eqs. (17), (18), (19), and (20) into Eqs. (12), (13), and (14) and by equating the corresponding coefficients of  $\varepsilon$  ( $\varepsilon \ll 1$ ) for different powers of  $\varepsilon$ , we can obtain the set of ordinary differential equations:

$$(1 + 6\Delta_1 u_0'^2) u_0'' - M^2 u_0 + \lambda_0 = 0, \tag{21}$$

$$(1 + i\gamma + 6\Delta_1 u_0'^2) u_1'' + 12\Delta_1 u_0' u_0'' u_1' - (M^2 + iH^2) u_1 + \lambda_1 = 0, \tag{22}$$

$$\left(1 + \frac{4Rd}{3}\right) \frac{1}{H^2 Pr} \theta_0'' + \frac{Nt}{H^2} \theta_0'^2 + \frac{Nb}{H^2} \phi_0' \theta_0' + \frac{Q}{H^2} \theta_0 + 2 \frac{Ec}{H^2} \Delta_1 u_0'^4 + \frac{Ec}{H^2} u_0'^2 + \frac{Ec}{H^2} M^2 u_0^2 = 0, \tag{23}$$

$$\left(1 + \frac{4Rd}{3}\right) \frac{1}{H^2 Pr} \theta_1'' + 2 \frac{Nt}{H^2} \theta_0' \theta_1' + \frac{Nb}{H^2} (\phi_0' \theta_1' + \theta_0' \phi_1') + \left(\frac{Q}{H^2} - i\right) \theta_1 + 8 \frac{Ec}{H^2} \Delta_1 u_0'^3 u_1' + 2 \frac{Ec}{H^2} u_0' u_1' + 2 \frac{Ec}{H^2} M^2 u_0 u_1 = 0, \tag{24}$$

$$\frac{1}{H^2 Pr Le} \phi_0'' + \frac{1}{H^2 Pr Le} \frac{Nt}{Nb} \theta_0'' - \frac{\gamma_1}{H^2} \phi_0 - \frac{K_1}{H^2} = 0, \tag{25}$$

$$\frac{1}{H^2 Pr Le} \phi_1'' + \frac{1}{H^2 Pr Le} \frac{Nt}{Nb} \theta_1'' - \left(\frac{\gamma_1}{H^2} + i\right) \phi_1 = 0. \tag{26}$$

The primes denote differentiation with respect to  $y$ .

The appropriate B.C.s are

$$u_0(0) = 0, u_1(0) = 0, \theta_0(0) = 0, \theta_1(0) = 0, \phi_0(0) = 0, \phi_1(0) = 0, \tag{27}$$

$$u_0(1) = 0, u_1(1) = 0, \theta_0(1) = 1, \theta_1(1) = 0, \phi_0(1) = 1, \phi_1(1) = 0. \tag{28}$$

Further, the dimensionless Nusselt (Nu) and Sherwood (Sh) numbers, i.e., heat transfer rate and mass transfer rate, respectively, at the channel walls are defined as follows:

$$Nu = \left(1 + \frac{4Rd}{3}\right) (\theta_0' + \varepsilon \theta_1' e^{it})_{y=0,1}, \quad Sh = (\phi_0' + \varepsilon \phi_1' e^{it})_{y=0,1}. \tag{29}$$

The shooting technique with the aid of Runge–Kutta fourth-order scheme is employed to solve the set of ODEs (21)–(26) with the B.C.s (27)–(28). The solution criteria for convergence are set to  $1 \times 10^{-10}$  precision, and the step size is fixed with 0.001 (i.e.,  $\Delta y = 0.001$ ).

### 3.1 Analysis of entropy generation

Entropy generation is calculated with the aid of thermodynamics second law and is defined as [34, 37].

Local entropy generation rate (EG) = mass and heat transfer irreversibility + fluid friction irreversibility + Joule heating irreversibility.

$$EG = \frac{k_f}{T_1^2} \left[ \left(1 + \frac{16\sigma^* T_1^3}{3\kappa^* k_f}\right) \left(\frac{\partial T^*}{\partial y^*}\right)^2 + \frac{\sigma_f B_0^2}{T_1} u^{*2} + \frac{\mu_f}{T_1} \left(\frac{\partial u^*}{\partial y^*}\right)^2 + \frac{\beta_3}{T_1} \left(\frac{\partial u^*}{\partial y^*}\right)^4 + \frac{D_B}{C_1^2} \left(\frac{\partial C^*}{\partial y^*}\right)^2 + \frac{D_B}{C_1 T_1} \left(\frac{\partial C^*}{\partial y^*}\right) \left(\frac{\partial T^*}{\partial y^*}\right) \right]. \tag{30}$$

Using Eq. (11) in Eq. (30), the non-dimensional local entropy generation rate is

$$\frac{EG}{EG_0} = \left(1 + \frac{4Rd}{3}\right) \left(\frac{\partial \theta}{\partial y}\right)^2 + \frac{M^2 Ec Pr}{\delta} u^2 + \frac{Ec Pr}{\delta} \left(\frac{\partial u}{\partial y}\right)^2 + \frac{2\Delta_1 Ec Pr}{\delta} \left(\frac{\partial u}{\partial y}\right)^4 + \Lambda \left(\frac{\xi}{\delta}\right)^2 \left(\frac{\partial \phi}{\partial y}\right)^2 + \Lambda \left(\frac{\xi}{\delta}\right) \left(\frac{\partial \phi}{\partial y}\right) \left(\frac{\partial \theta}{\partial y}\right), \tag{31}$$

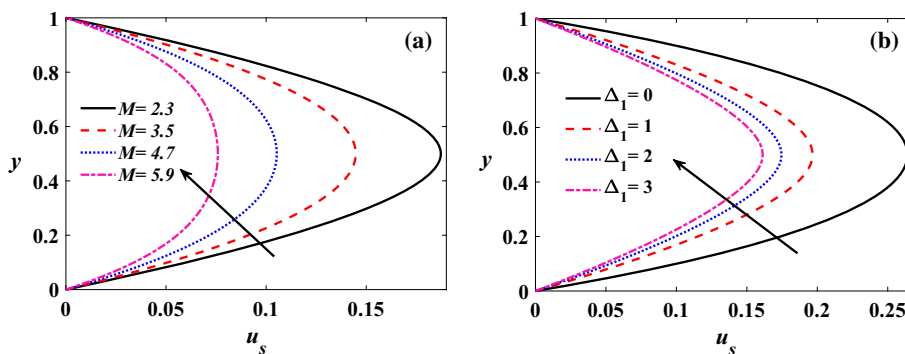
here,  $EG_0 = \frac{k_f}{T_1^2} \left(\frac{T_1 - T_0}{h}\right)^2$  is characteristic entropy generation rate,  $\delta = \frac{T_1 - T_0}{T_1}$  is temperature difference,  $\xi = \frac{C_1 - C_0}{C_1}$  is concentration difference, and  $\Lambda = \frac{D_B}{k_f}$ . The entropy generation rate (NG) =  $\frac{EG}{EG_0}$ .

$$NG = \left(1 + \frac{4Rd}{3}\right) \left(\frac{\partial \theta}{\partial y}\right)^2 + \frac{M^2 Ec Pr}{\delta} u^2 + \frac{Ec Pr}{\delta} \left(\frac{\partial u}{\partial y}\right)^2 + \Lambda \left(\frac{\xi}{\delta}\right)^2 \left(\frac{\partial \phi}{\partial y}\right)^2 + \frac{2\Delta_1 Ec Pr}{\delta} \left(\frac{\partial u}{\partial y}\right)^4 + \Lambda \left(\frac{\xi}{\delta}\right) \left(\frac{\partial \phi}{\partial y}\right) \left(\frac{\partial \theta}{\partial y}\right). \tag{32}$$

**Table 1** Comparison of present results with NDSolve at  $y = 0$  when  $H = 3, M = 2, \Delta_1 = 1, Pr = 21, Ec = 1, Nb = 0.5, Nt = 0.5, Rd = 2, t = \pi/3, \lambda_0 = 3, \lambda_1 = 2, \gamma = 1, \gamma_1 = 1, Le = 1, K_1 = 0.001, Q = -0.5,$  and  $\varepsilon = 0.1$

Parameter	Values	Present results		NDSolve	
		Nu	Sh	Nu	Sh
$M$	2.3	20.0024676348	- 3.1130298998	20.0024761653	- 3.1130322187
	3.5	18.8385898451	- 2.8424915165	18.8386290385	- 2.8425019269
	4.7	17.4715666286	- 2.5461306202	17.4715709334	- 2.5461318722
$\Delta_1$	1	20.2092541117	- 3.1647550976	20.2092673390	- 3.1647600833
	2	19.1643956401	- 2.9444497841	19.1643955884	- 2.9444497738
	3	18.5642139668	- 2.8183275108	18.563358915	- 2.8183269530
$Nt$	0.2	10.7868678222	- 0.3929965886	10.7869620538	- 0.3930060945
	0.4	16.3607795081	- 1.8175350682	16.3607811517	- 1.8175354085
	0.6	24.8583539808	- 5.1225858767	24.8583538098	- 5.1225858301

**Fig. 2** Steady velocity profiles: **a** effect of  $M$ , **b** effect of  $\Delta_1$



Bejan number (Be) =  $\frac{\text{Heat and mass transfer irreversibility}}{\text{Entropy generation rate}}$ .

$$Be = \frac{\left(1 + \frac{4Rd}{3}\right) \left(\frac{\partial \theta}{\partial y}\right)^2 + \Lambda \left(\frac{\xi}{\delta}\right)^2 \left(\frac{\partial \phi}{\partial y}\right)^2 + \Lambda \left(\frac{\xi}{\delta}\right) \left(\frac{\partial \phi}{\partial y}\right) \left(\frac{\partial \theta}{\partial y}\right)}{NG} \tag{33}$$

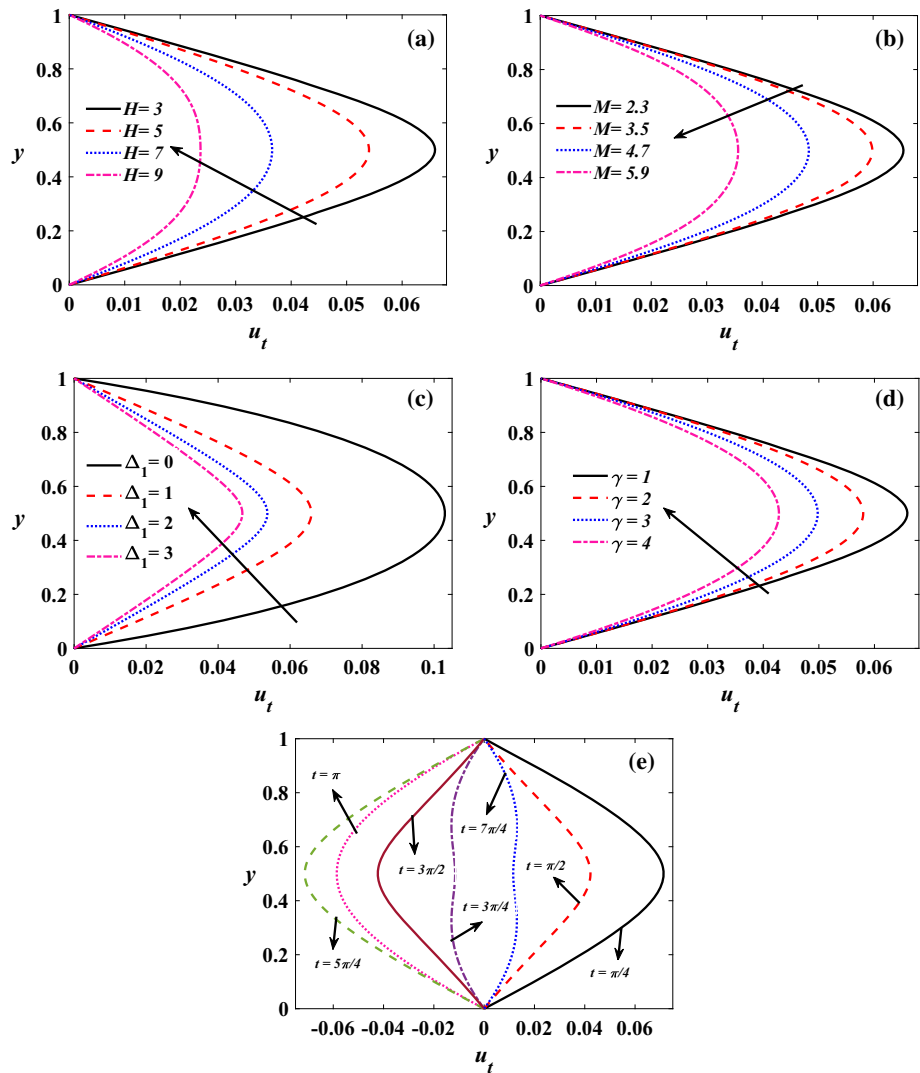
Table 1 presents the comparison between the present results and results obtained by NDSolve. To examine the rationality of the current model, we analyzed the outcomes of this work using two different inbuilt mathematical software due to the lack of experimental studies related to present model. The resulting table values reveal that there exists a good agreement in between the outcomes.

### 4 Results and discussion

The variations in the pertinent physical parameters on flow variables are deliberated through the detailed graphical illustration in this section. Figures 2, 3, 4, 5, 6, 7, 8, and 9 depict the variations of non-Newtonian parameter ( $\Delta_1$ ), Hartmann number ( $M$ ), material parameter ( $\gamma$ ), Eckert number ( $Ec$ ), frequency parameter ( $H$ ), Radiation parameter ( $Rd$ ), Brownian motion parameter ( $Nb$ ), thermophoresis parameter ( $Nt$ ), heat source/sink parameter ( $Q$ ), chemical reaction parameter ( $\gamma_1$ ), Lewis number ( $Le$ ) on velocity, temperature, concentration of nanoparticles, entropy generation ( $NG$ ), and Bejan number ( $Be$ ) of third grade nanofluid. To investigate the effect of various physical parameters, the values of pertinent parameters are taken based on the literature survey as  $M = 2, Pr = 21, Ec = 1, H = 3, Rd = 2, \gamma = 1, \Delta_1=1, \lambda_0 = 3, \lambda_1 = 2, Nb = 0.5, Nt = 0.5, Q = -0.5, \gamma_1=1, t = \pi/3, Le = 1, K_1=0.001, \Lambda=0.1, \delta=0.1, \xi=0.15, \varepsilon=0.1$ . Figure 2a, b shows the impacts of Hartmann number and non-Newtonian parameter on the steady velocity ( $u_s$ ) of third grade nanoliquid in a channel. Figure 2a depicts that  $u_s$  is declined by augmenting the Hartmann number. When magnetic field is applied to the nanofluid flow creates a resistance drag force called Lorentz forces (retarding forces) that oppose the flow direction. A similar nature can be seen in Fig. 2b for rising values of non-Newtonian parameter because magnifying the non-Newtonian parameter supports the viscoelasticity which reduces the velocity of the flow.

The unsteady velocity ( $u_t$ ) profiles of third grade nanoliquid are portrayed in Fig. 3a–e. These figures illustrate the effects of  $H, M, \Delta_1, \gamma,$  and  $t$  on the unsteady velocity. Intensifying  $H$  escalates the height of the oscillations, due to this  $u_t$  slows down with the enhancement of  $H$  (see Fig. 3a). The effect of Hartmann number on flow velocity is presented in Fig. 3b which reveals that  $u_t$  is decelerated for rising values of  $M$  because the applied magnetic field creates resistance drag forces that opposes the flow direction.

**Fig. 3** Unsteady velocity profiles: **a** effect of  $H$ , **b** effect of  $M$ , **c** effect of  $\Delta_1$ , **d** effect of  $\gamma$ , **e** effect of  $t$

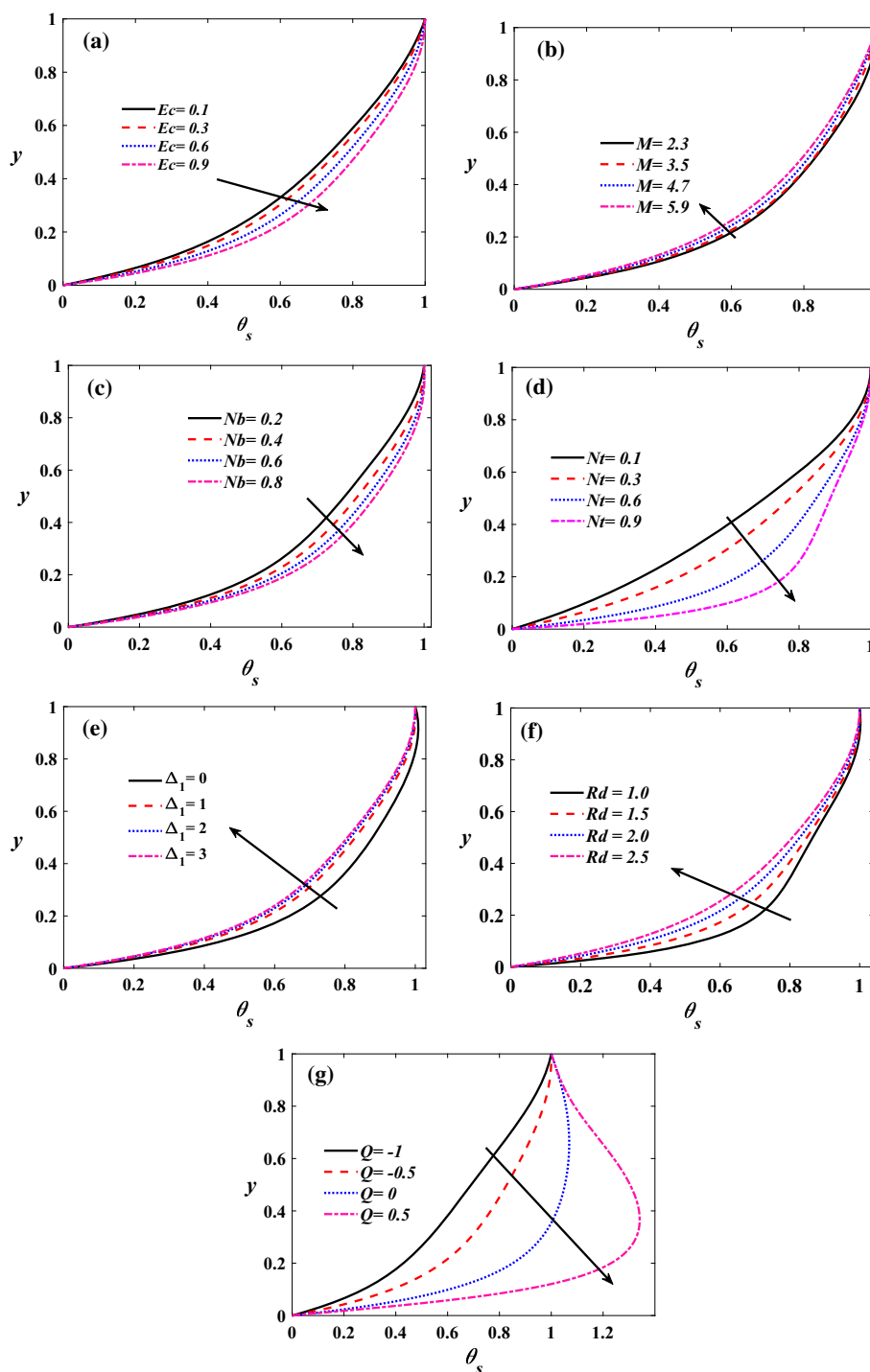


The influence of non-Newtonian and material parameters on velocity is displayed in Fig. 3c–d. From these figures, one can infer that magnifying the non-Newtonian and material parameters reduce the velocity because the viscoelasticity of the nanofluid rises for the higher values of  $\Delta_1$  and  $\gamma$  which declines the velocity. The impact of time on velocity profile is depicted in Fig. 3e which shows that there is an oscillating behavior in  $u_t$  for various values of time, and the supreme is near the center of the channel.

The steady temperature profiles ( $\theta_s$ ) of third grade nanofluid are depicted in Fig. 4a–g and shown the effects of viscous dissipation, Hartmann number, Brownian motion parameter, thermophoresis parameter, non-Newtonian parameter, radiation parameter, and heat source/sink parameter. Figure 4a presents that enhancement in Eckert number upsurses  $\theta_s$ . Since the  $Ec$  is defined as the ratio of heat enthalpy to kinetic energy particles, enhancing the values of Eckert number reduce the heat enthalpy factors by enhancing the kinetic energy particles that result a rise in temperature. The opposite behavior can be seen in Fig. 4b for the escalation of Hartmann number. Since the velocity of the nanofluid is declined for rising values of  $M$  leads that the thermal energy transportation due to advection is declined from the channel walls to the fluid region. Figure 4c reveals that  $\theta_s$  is accelerated for a rise in Brownian motion parameter because intensifying  $Nb$  boosts the random speed of nanoparticles in the fluid domain that produces additional energy by collide between fluid molecules and particles as results gain in temperature. The similar nature can be found by enhancing the thermophoresis parameter (see Fig. 4d). Since the thermophoresis parameter involves a temperature gradient that supports the energy particles to transport the energy from high-level temperature place to low-level temperature area. Figure 4e displays that  $\theta_s$  is diminishing for the escalation of non-Newtonian parameter due to a rise in viscoelasticity. Figure 4f illustrates that an increment in radiation parameter causes a decrement in temperature of the nanofluid because the thermal boundary layer thickness becomes thinner for higher values of radiation parameter. Figure 4g elucidates that  $\theta_s$  upsurses for growing values of heat source parameter ( $Q > 0$ ), whereas the opposite behavior can be noticed for rising values of heat sink parameter ( $Q < 0$ ).

The unsteady temperature profiles ( $\theta_t$ ) of third grade nanofluid are portrayed in Fig. 5a–g. These figures present the effects of  $H$ ,  $M$ ,  $Ec$ ,  $Nb$ ,  $Nt$ ,  $Rd$ , and  $t$  on  $\theta_t$ . Figure 5a reveals that intensifying the frequency parameter tend to cause an oscillating character in

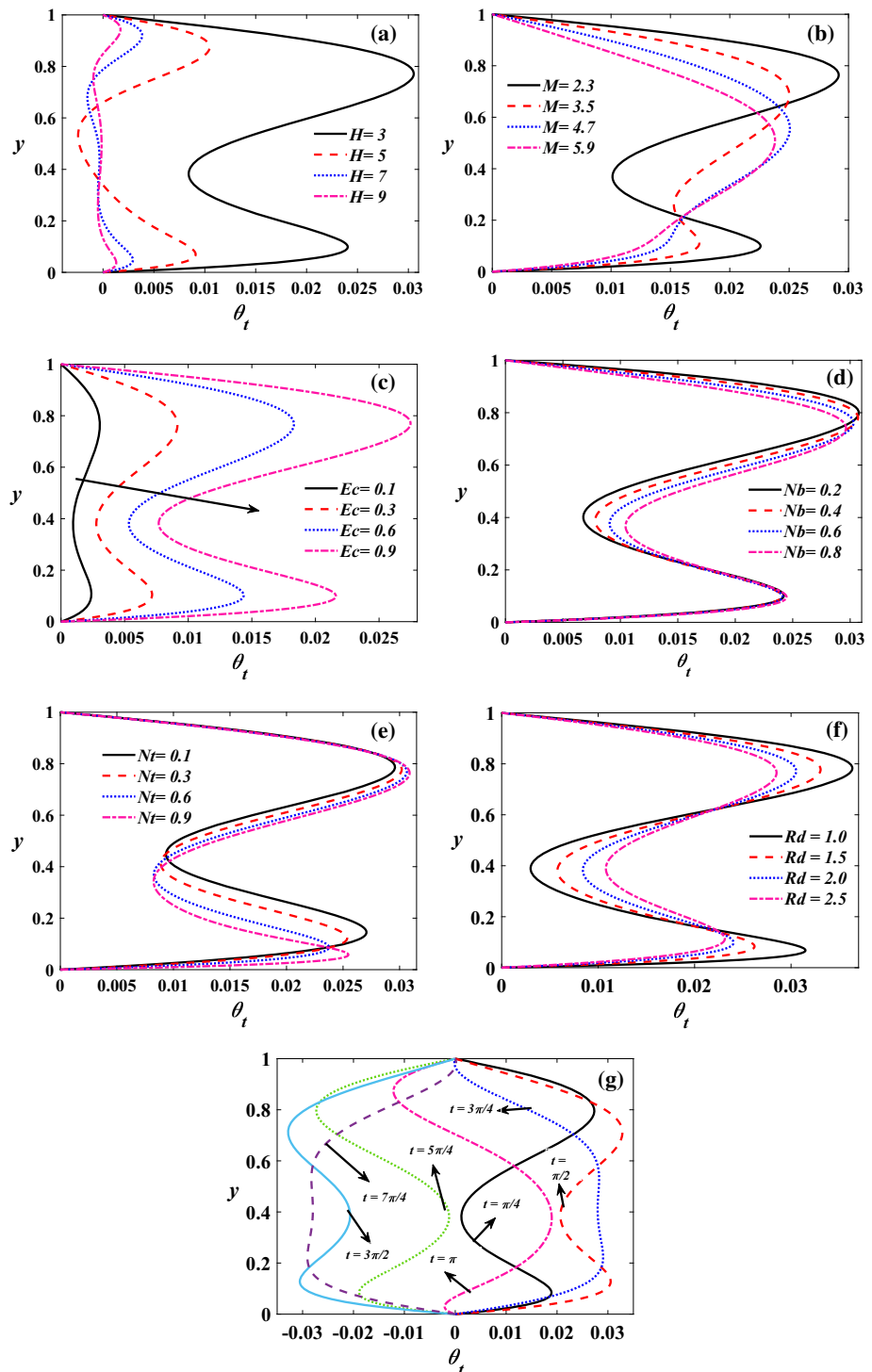
**Fig. 4** Steady temperature profiles: **a** effect of  $Ec$ , **b** effect of  $M$ , **c** effect of  $Nb$ , **d** effect of  $Nt$ , **e** effect of  $\Delta_1$ , **f** effect of  $Rd$ , **g** effect of  $Q$



$\theta_t$ , and the supreme is near to the upper wall. A similar nature is observed for the higher values of  $M$  on  $\theta_t$  (see Fig. 5b). The impact of Eckert number on  $\theta_t$  is presented in Fig. 5c. From this figure, one can infer that magnifying the  $Ec$  accelerates the temperature of nanofluid and the supreme is found near to the upper wall. Accelerating Brownian motion parameter and thermophoresis parameter show a wavering nature in  $\theta_t$  due to the random movement of particles (see Fig. 5d, e). Figure 5f displays the impact of radiation parameter on  $\theta_t$ . From the same figure, one can find that there is a wavering character in  $\theta_t$  for the higher values of  $Rd$ . For various  $t$  values, there exists an oscillating behavior in  $\theta_t$  and the maximum temperature is near the center of the channel (see Fig. 5g).

Figure 6a–d presents the impact of chemical reaction parameter, Lewis number, Brownian motion parameter, and thermophoresis parameter on steady nanoparticles concentration ( $\phi_s$ ). Figure 6a depicts that the concentration of nanoparticles decelerating for augmenting values of chemical reaction parameter. A similar nature is observed by upsurging Lewis number on  $\phi_s$  because the rate

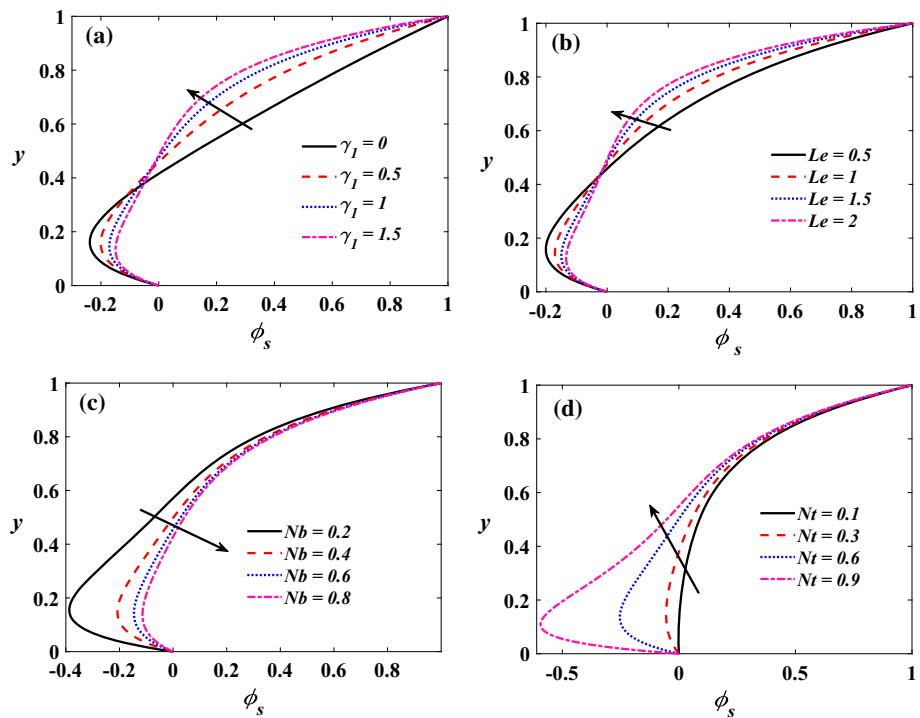
**Fig. 5** Unsteady temperature profiles: **a** effect of  $H$ , **b** effect of  $M$ , **c** effect of  $Ec$ , **d** effect of  $Nb$ , **e** effect of  $Nt$ , **f** effect of  $Rd$ , **g** effect of  $t$



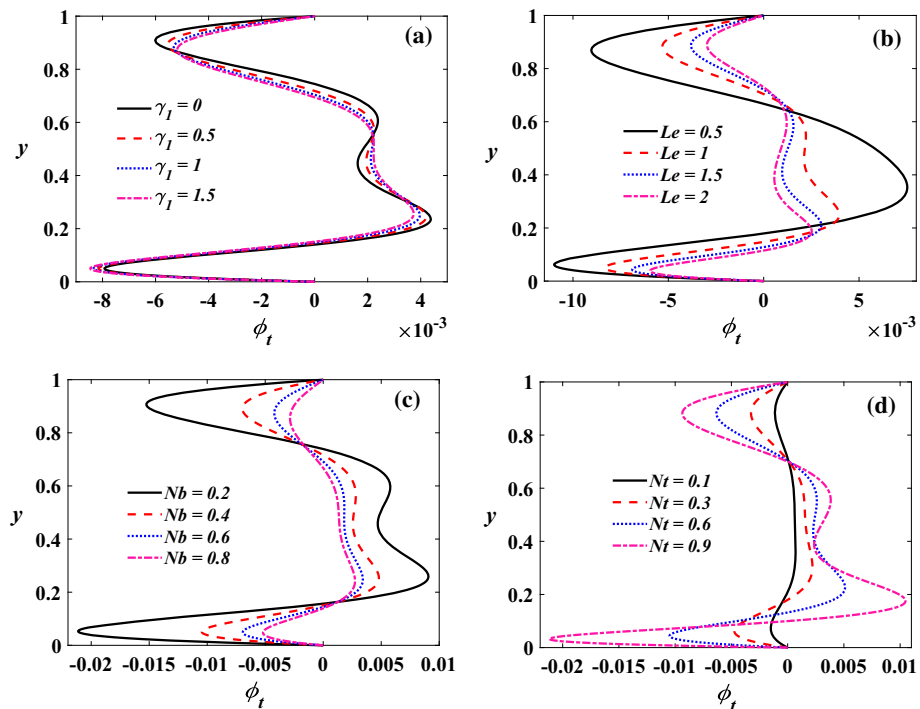
of mass transfer is improved for high values of  $Le$  that reduces the nanoparticles concentration (see Fig. 6b). Figure 6c illustrates the concentration profiles for the Brownian motion parameter. From this figure, one can infer that accelerating  $Nb$  enhances the concentration of nanoparticles due to the random movement of particles helps to move particles in an entire fluid domain which boosts  $\phi_s$ , whereas the reverse trend is noticed for rising values of  $Nt$  on  $\phi_s$  (see Fig. 6d). The unsteady concentration profiles ( $\phi_t$ ) are depicted in Fig. 7a–d, and these figures show the effects of  $\gamma_1$ ,  $Le$ ,  $Nb$ , and  $Nt$  on  $\phi_s$ . Figure 7a displays that an increment in  $\gamma_1$  shows the oscillating character in  $\phi_t$ . The similar kind of nature can be found in  $\phi_t$  for growing values of  $Le$ ,  $Nb$ , and  $Nt$  (Fig. 7b–d).

Figure 8a–f elucidates the effects of dimensionless parameters  $Rd$ ,  $M$ ,  $Ec$ ,  $\delta$ ,  $\Delta_1$ , and  $\xi$  on entropy generation rate (NG). Figure 8a reveals that magnifying the radiation parameter accelerates the entropy generation because augmenting  $Rd$  boosts the

**Fig. 6** Steady concentration profiles: **a** effect of  $\gamma_1$ , **b** effect of  $Le$ , **c** effect of  $Nb$ , **d** effect of  $Nt$

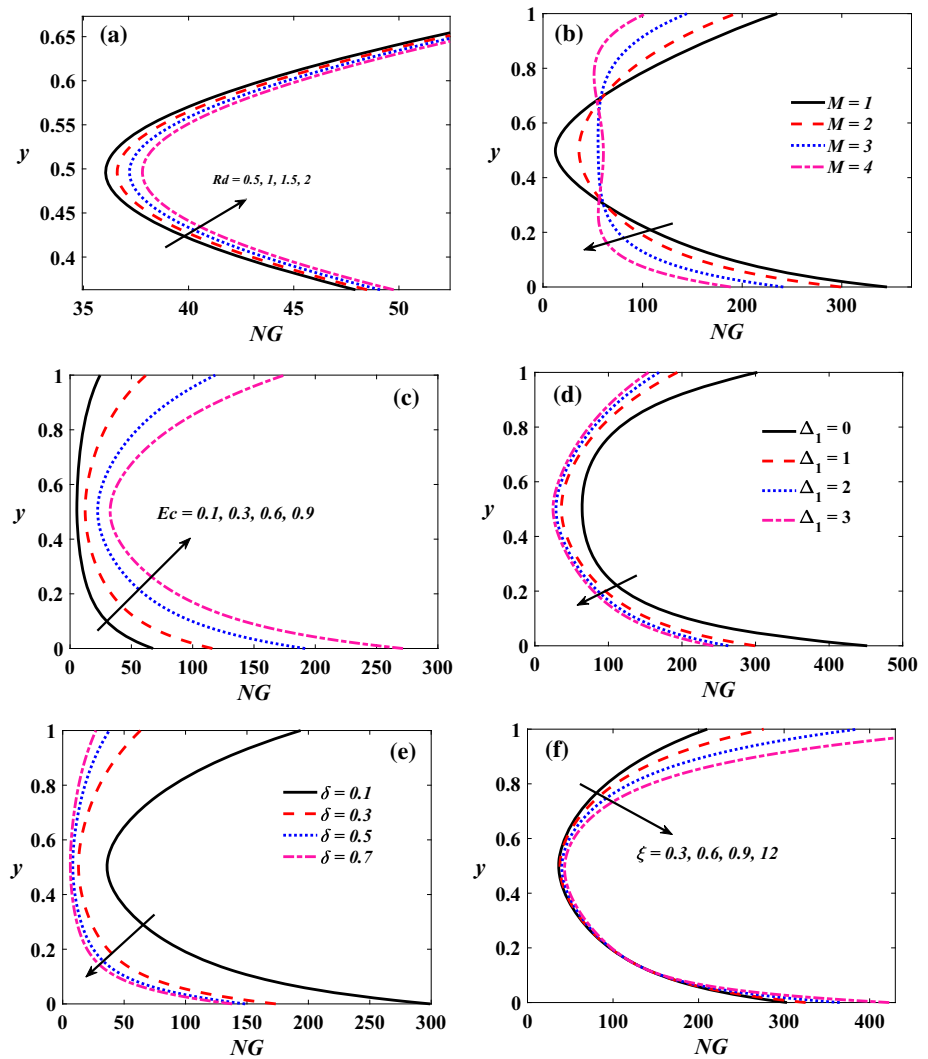


**Fig. 7** Unsteady concentration profiles: **a** effect of  $\gamma_1$ , **b** effect of  $Le$ , **c** effect of  $Nb$ , **d** effect of  $Nt$



thermal conductivity of the nanofluid. Figure 8b displays the impression of  $M$  on NG. From this figure, one can found that the entropy generation rate is decreasing at channel walls for rising values of  $M$ . Since the flow is applied by the magnetic field produces the Lorentz forces as a result entropy reduces. Figure 8c depicts that the entropy generation upsurges with the enhancement of viscous dissipation due to the frictional heating between fluid molecules and particles with channel walls. The opposite nature is elucidated for rising values of non-Newtonian parameter because the viscoelasticity rises for higher values of  $\Delta_1$  (see Fig. 8d). Figure 8e illustrates that an enhancement in the temperature difference reduces the entropy generation, whereas intensifying the nanoparticle concentration difference accelerates the entropy generation rate (see Fig. 8f).

**Fig. 8** Entropy production: **a** effect of  $Rd$ , **b** effect of  $M$ , **c** effect of  $Ec$ , **d** effect of  $\Delta_1$ , **e** effect of  $\delta$ , **f** effect of  $\xi$



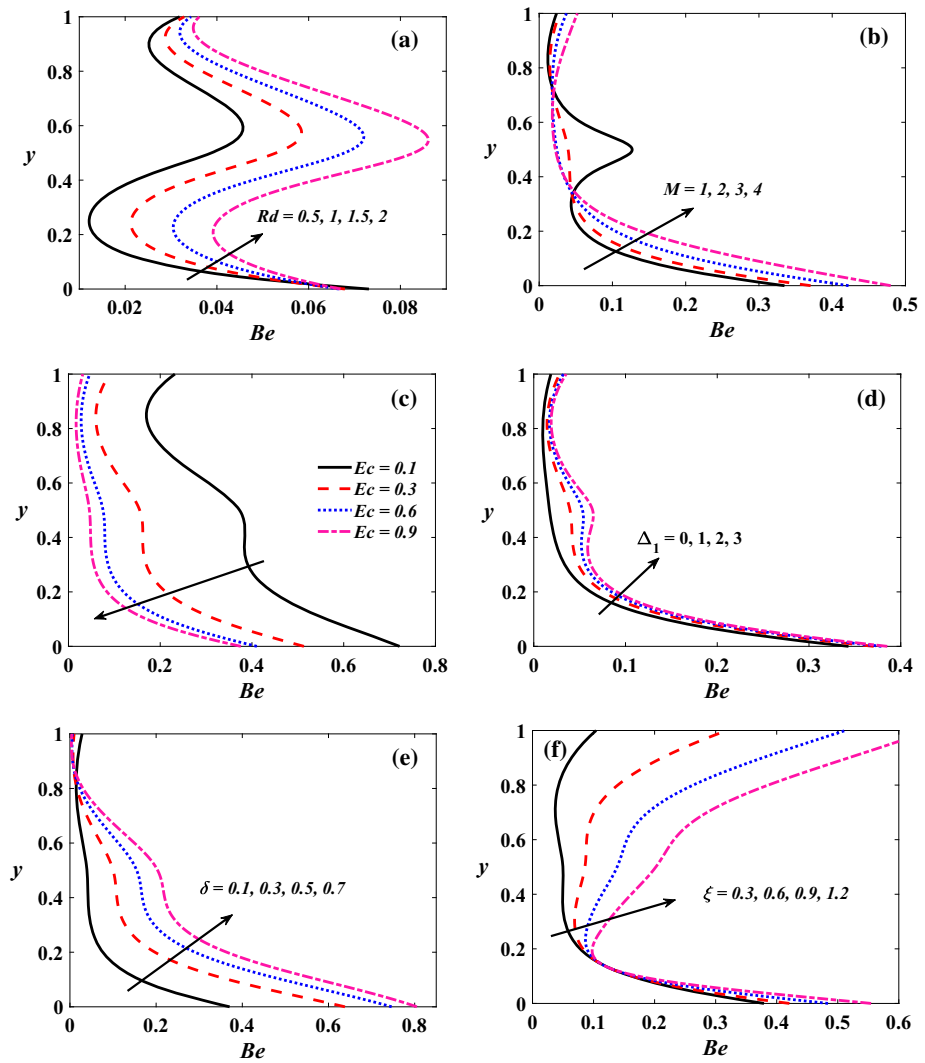
The impressions of dimensionless parameters of  $Rd$ ,  $M$ ,  $Ec$ ,  $\Delta_1$ ,  $\delta$ , and  $\xi$  on Bejan number ( $Be$ ) are presented in Fig. 9a–f. Intensifying radiation parameter accelerates the Bejan number, and the profiles show the wavering nature (see Fig. 9a). Figure 9b clarifies that improving the Hartmann number accelerates the Bejan number owing to the Lorentz forces, i.e., delaying forces created by an applied magnetic field. Figure 9c depicts that enhancing viscous dissipation reduces the Bejan number due to the frictional forces in the fluid domain. Augmenting the non-Newtonian parameter accelerates the Bejan number (see Fig. 9d). The similar behavior can be noticed for the upsurging values of  $\delta$  and  $\xi$  (see Fig. 9e, f).

Table 2 shows the Nusselt number ( $Nu$ ) and Sherwood number ( $Sh$ ) distributions for different parameter values of  $M$ ,  $\Delta_1$ ,  $Ec$ ,  $Nb$ ,  $Nt$ , and  $Rd$  at lower wall. From the tabulated values, one can observe that the rate of heat transfer is accelerated for the higher values in Eckert number, Brownian motion, and thermophoresis parameter, while  $Nu$  is reduced for escalation values of  $M$ ,  $\Delta_1$ , and  $Rd$ . Further, from the same Table, it is clearly noticed that a rise in  $M$ ,  $\Delta_1$ ,  $Nb$ , and  $Rd$  intensifies the mass transfer rate, whereas magnifying the values of  $Ec$  and  $Nt$  slow down the mass transfer rate of the third grade nanoliquid.

### 5 Conclusion

In the present study, the MHD pulsating flow of third grade nanofluid in a channel with Brownian motion, thermophoresis, Joule heating impacts has been analyzed. The analysis of entropy generation is performed and used the Buongiorno model for nanofluids. The results of this study could be useful in several fields such as biomedical engineering, manufacturing industries as coolants, energy conservation, pressure surges, dynamics of physiological fluids, biomedicines, and nano-drug suspension in pharmaceuticals. The perturbation technique is employed on flow governing equations (PDEs) to convert into a set of ODEs. The shooting process along with the support of Runge–Kutta fourth-order method is utilized to solve the set of ODEs. The effects of dimensionless

**Fig. 9** Bejan number distribution profiles: **a** effect of  $Rd$ , **b** effect of  $M$ , **c** effect of  $Ec$ , **d** effect of  $\Delta_1$ , **e** effect of  $\delta$ , **f** effect of  $\xi$



emerging physical parameters and pertinent variables are discussed using graphical presentations. The main investigated outcomes are summarized as follows:

- Accelerating the non-Newtonian parameter, Hartmann number, frequency parameter, and material parameter decline the velocity.
- Enhancement in viscous dissipation, heat source parameter, Brownian motion parameter, and thermophoresis enhances the steady temperature of the nanofluid, while the temperature reduces for the higher values of  $M$  and  $Rd$ .
- The unsteady temperature distributions of  $Ec$ ,  $Rd$ ,  $M$ ,  $H$ ,  $Nb$ , and  $Nt$  show the oscillating behavior.
- Augmenting the chemical reaction parameter, Lewis number, and thermophoresis parameter decelerate the steady concentration of nanoparticles, whereas a rise in Brownian motion parameter encourages the nanoparticles concentration.
- The entropy generation rate enhances with a rise in  $Rd$ ,  $Ec$ , and  $\xi$ , whereas the entropy generation rate declines for high values of  $M$ ,  $\Delta_1$ , and  $\delta$ .
- Intensifying  $Rd$ ,  $M$ ,  $\xi$ ,  $\Delta_1$ , and  $\delta$  encourage the Bejan number.
- A rise in Eckert number, Brownian motion parameter, and thermophoresis parameter enhances the heat transfer rate.

**Table 2** Variations in heat and mass transfer rates at  $y = 0$  for various physical parameters when  $H = 3, M = 2, \Delta_1 = 1, Pr = 21, Ec = 1, Nb = 0.5, Nt = 0.5, Rd = 2, t = \pi/3, \lambda_0 = 3, \lambda_1 = 2, \gamma = 1, \gamma_1 = 1, Le = 1, K_1 = 0.001, Q = -0.5,$  and  $\varepsilon = 0.1$

Parameter	Values	At bottom wall $y = 0$	
		Nu	Sh
$M$	2.3	20.0024676348	- 3.1130298998
	3.5	18.8385898451	- 2.8424915165
	4.7	17.4715666286	- 2.5461306202
$\Delta_1$	1	20.2092541117	- 3.1647550976
	2	19.1643956401	- 2.9444497841
	3	18.5642139668	- 2.8183275108
$Ec$	0.1	13.4220059635	- 1.7408784583
	0.3	14.8252262901	- 2.0321053024
	0.6	17.0384921239	- 2.4949033338
$Nb$	0.1	16.7810369158	- 12.7479326406
	0.3	18.6064976246	- 4.7915146408
	0.6	20.9391132677	- 2.7480535579
$Nt$	0.2	10.7868678222	- 0.3929965886
	0.4	16.3607795081	- 1.8175350682
	0.6	24.8583539808	- 5.1225858767
$Rd$	0	29.8138146928	- 26.2774103188
	0.5	25.9660193757	- 12.4136209534
	1	23.0524037488	- 7.0538587661

- Sherwood number is accelerated for the higher values of  $M, \Delta_1, Nb,$  and  $Rd.$

**Data Availability Statement** This manuscript has no associated data.

**Declarations**

**Conflict of interest** The authors have declared that there is no conflict of interest.

**References**

1. R.R. Souza, M.I. Goncalves, O.R. Rodrigues, G. Minas, J.M. Miranda, L.N.A. Moreira, R. Lima, G. Coutinho, J.E. Pereira, S.A. Moita, Recent advances on the thermal properties and applications of nanofluids: From nanomedicine to renewable energies. *Appl. Therm. Eng.* **201**, 117725 (2022)
2. A.J. Chamkha, A.M. Rashad, M.A. Mansour, T. Armaghani, M. Ghalambaz, Effects of heat sink and source and entropy generation on MHD mixed convection of a Cu-water nanofluid in a lid-driven square porous enclosure with partial slip. *Phys. Fluids.* **10**(1063/1), 4981911 (2017)
3. S.U.S. Choi, J.A. Eastman, Enhancing thermal conductivity of fluids with nanoparticles. *Am. Soc. Mech. Eng. Fluids Eng. Div. FED* **231**, 99–105 (1995)
4. J. Buongiorno, Convective transport in nanofluids. *J. Heat Transf.* **128**, 240–250 (2006). <https://doi.org/10.1115/1.2150834>
5. Z. Shah, T. Gul, S. Islam, M.A. Khan, E. Bonyah, F. Hussain, S. Mukhtar, M. Ullah, Three dimensional third grade nanofluid flow in a rotating system between parallel plates with Brownian motion and thermophoresis effects. *Results Phys.* **10**, 36–45 (2018). <https://doi.org/10.1016/j.rinp.2018.05.020>
6. C.K. Kumar, S. Srinivas, A. Subramanyam Reddy, MHD pulsating flow of Casson nanofluid in a vertical porous space with thermal radiation and Joule heating. *J. Mech.* **36**, 535–549 (2020). <https://doi.org/10.1017/jmech.2020.5>
7. T. Hayat, R. Riaz, A. Aziz, A. Alsaedi, Influence of Arrhenius activation energy in MHD flow of third grade nanofluid over a nonlinear stretching surface with convective heat and mass conditions. *Phys. A Stat. Mech. Appl.* **549**, 124006 (2020). <https://doi.org/10.1016/j.physa.2019.124006>
8. R. Naz, S. Tariq, M. Sohail, Z. Shah, Investigation of entropy generation in stratified MHD Carreau nanofluid with gyrotactic microorganisms under Von Neumann similarity transformations. *Eur. Phys. J. Plus.* **135**, 1–22 (2020). <https://doi.org/10.1140/epjp/s13360-019-00069-0>
9. Y.-M. Chu, M.I. Khan, B.N. Khan, S. Kadry, S.U. Khan, Significance of activation energy, bio-convection and magnetohydrodynamic in flow of third grade fluid (non-Newtonian) towards stretched surface: A Buongiorno model analysis. *Int. Commun. Heat Mass Transf.* **118**, 104893 (2020)
10. M. Derikvand, M.S. Solari, D. Toghraie, Numerical investigation of the effect of a porous block and flow injection using non-Newtonian nanofluid on heat transfer and entropy generation in a microchannel with hydrophobic walls. *Eur. Phys. J. Plus.* (2021). <https://doi.org/10.1140/epjp/s13360-021-01846-6>
11. S.A. Khan, T. Hayat, A. Alsaedi, Cattaneo Christov (CC) heat and mass fluxes in Stagnation point flow of Jeffrey nanoliquids by a stretched surface. *Chinese. J. Phys.* **76**, 205–216 (2022). <https://doi.org/10.1016/j.cjph.2021.11.034>
12. M. Hatami, J. Hatami, D.D. Ganji, Computer simulation of MHD blood conveying gold nanoparticles as a third grade non-Newtonian nanofluid in a hollow porous vessel. *Comput. Methods Programs Biomed.* **113**, 632–641 (2014). <https://doi.org/10.1016/j.cmpb.2013.11.001>

13. A. Sinha, MHD flow and heat transfer of a third order fluid in a porous channel with stretching wall: Application to hemodynamics. *Alex. Eng. J.* **54**, 1243–1252 (2015)
14. J. Rana, P.V.S.N. Murthy, Solute dispersion in pulsatile Casson fluid flow in a tube with wall absorption. *J. Fluid Mech.* **793**, 877–914 (2016). <https://doi.org/10.1017/jfm.2016.155>
15. S. Rajamani, A. Subramanyam Reddy, Pulsating flow of electrically conducting couple stress nanofluid in a channel with ohmic dissipation and thermal radiation—dynamics of blood. *Proc. Inst. Mech. Eng. Part E J. Process Mech. Eng.* **235**, 1895–1909 (2021). <https://doi.org/10.1177/09544089211025177>
16. T. Hussain, T. Hayat, S.A. Shehzad, A. Alsaedi, B. Chen, A model of solar radiation and joule heating in flow of third grade nanofluid. *Z. Naturforsch. Sect. J. Phys. Sci.* **70**, 177–184 (2015). <https://doi.org/10.1515/zna-2014-0267>
17. A. Abbasi, W. Farooq, T. Muhammad, M.I. Khan, S.U. Khan, F. Mabood, S. Bibi, Implications of the third-grade nanomaterials lubrication problem in terms of radiative heat flux: a Keller box analysis. *Chem. Phys. Lett.* **2021**, 139041 (2021). <https://doi.org/10.1016/j.cplett.2021.139041>
18. M. Ben Henda, H. Waqas, M. Hussain, S.U. Khan, W. Chammam, S.A. Khan, I. Tlili, Applications of activation energy along with thermal and exponential space-based heat source in bioconvection assessment of magnetized third grade nanofluid over stretched cylinder/sheet. *Case Stud. Therm. Eng.* **26**, 101043 (2021). <https://doi.org/10.1016/j.csite.2021.101043>
19. Y.J. Xu, S.U. Khan, K. Al-Khaled, M.I. Khan, F. Alzahrani, M.I. Khan, Effectiveness of induced magnetic force and non-uniform heat source/sink features for enhancing the thermal efficiency of third grade nanofluid containing microorganisms. *Case Stud. Therm. Eng.* **27**, 101305 (2021). <https://doi.org/10.1016/j.csite.2021.101305>
20. K. Govindarajulu, A. Subramanyam Reddy, Magnetohydrodynamic pulsatile flow of third grade hybrid nanofluid in a porous channel with Ohmic heating and thermal radiation effects. *Phys. Fluids.* **34**, 013105 (2022). <https://doi.org/10.1063/5.0074894>
21. C.Y. Wang, Pulsatile flow in a porous channel. *J. Appl. Mech. Trans.* **38**, 553–555 (1971). <https://doi.org/10.1115/1.3408822>
22. G. Radhakrishnamacharya, M.K. Maiti, Heat transfer to pulsatile flow in a porous channel. *Int. J. Heat Mass Transf.* **20**, 171–173 (1977)
23. N. Datta, D.C. Dalal, S.K. Mishra, Unsteady heat transfer to pulsatile flow of a dusty viscous incompressible fluid in a channel. *Int. J. Heat Mass Transf.* **36**, 1783–1788 (1993). [https://doi.org/10.1016/S0017-9310\(05\)80164-4](https://doi.org/10.1016/S0017-9310(05)80164-4)
24. T. Malathy, S. Srinivas, Pulsating flow of a hydromagnetic fluid between permeable beds. *Int. Commun. Heat Mass Transf.* **35**, 681–688 (2008). <https://doi.org/10.1016/j.icheatmasstransfer.2007.12.006>
25. H.M. Shawkly, Pulsatile flow with heat transfer of dusty magnetohydrodynamic Ree-Eyring fluid through a channel. *Heat Mass Transf.* **45**, 1261–1269 (2009). <https://doi.org/10.1007/s00231-009-0502-0>
26. M. Ebrahim Qomi, G.A. Sheikhzadeh, A. Fattahi, Heat transfer enhancement in a microchannel using a pulsating MHD hybrid nanofluid flow. *Energy Sources Part A Recover. Util. Environ. Eff.* (2020). <https://doi.org/10.1080/15567036.2020.1834031>
27. G. Venkatesan, A.S. Reddy, Joule heating impacts on MHD pulsating flow of Au/CuO-blood Oldroyd-B nanofluid in a porous channel. *Heat Transf.* **50**, 7495–7513 (2021). <https://doi.org/10.1002/htj.22240>
28. S. Ahmed, H. Xu, Forced convection with unsteady pulsating flow of a hybrid nanofluid in a microchannel in the presence of EDL, magnetic and thermal radiation effects. *Int. Commun. Heat Mass Transf.* **120**, 105042 (2021). <https://doi.org/10.1016/j.icheatmasstransfer.2020.105042>
29. A. Kardgar, Numerical investigation of MHD oscillating power-law non-Newtonian nanofluid flow in an enclosure. *Eur. Phys. J. Plus.* (2021). <https://doi.org/10.1140/epjp/s13360-020-01029-9>
30. D. Rajkumar, A. Subramanyam Reddy, Pulsating electrically conducting flow of Au/SWCNTs-blood micropolar nanofluid in a porous channel with Ohmic heating, thermal radiation. *Phys. Scr.* **96**, 125233 (2021). <https://doi.org/10.1088/1402-4896/ac2e81>
31. M. Hemmat Esfe, M. Bahiraei, A. Torabi, M. Valadkhani, A critical review on pulsating flow in conventional fluids and nanofluids: thermo-hydraulic characteristics. *Int. Commun. Heat Mass Transf.* **120**, 104859 (2021). <https://doi.org/10.1016/j.icheatmasstransfer.2020.104859>
32. G. Venkatesan, A.S. Reddy, Insight into the dynamics of blood conveying alumina nanoparticles subject to Lorentz force, viscous dissipation, thermal radiation, Joule heating, and heat source. *Eur. Phys. J. Spec. Top.* **230**, 1475–1485 (2021). <https://doi.org/10.1140/epjs/s11734-021-00052-w>
33. A. Bejan, A study of entropy generation in fundamental convective heat transfer. *J. Heat Transf.* **1979**, 718–725 (1979)
34. M.M. Rashidi, S. Bagheri, E. Momoniat, N. Freidoonimehr, Entropy analysis of convective MHD flow of third grade non-Newtonian fluid over a stretching sheet. *Ain Shams Eng. J.* **8**, 77–85 (2017). <https://doi.org/10.1016/j.asej.2015.08.012>
35. T. Hayat, S. Nawaz, A. Alsaedi, B. Ahmad, Entropy analysis for the peristaltic flow of third grade fluid with variable thermal conductivity. *Eur. Phys. J. Plus.* **135**, 1–18 (2020). <https://doi.org/10.1140/epjp/s13360-020-00421-9>
36. A.M. Rashad, M.A. Mansour, T. Armaghani, A.J. Chamkha, MHD mixed convection and entropy generation of nanofluid in a lid-driven U-shaped cavity with internal heat and partial slip. *Phys. Fluids.* **31**, 10 (2019). <https://doi.org/10.1063/1.5079789>
37. T. Hayat, R. Riaz, A. Aziz, A. Alsaedi, Analysis of entropy generation for MHD flow of third grade nanofluid over a nonlinear stretching surface embedded in a porous medium. *Phys. Scr.* **94**, 125703 (2019)
38. K. Loganathan, K. Mohana, M. Mohanraj, P. Sakthivel, S. Rajan, Impact of third-grade nanofluid flow across a convective surface in the presence of inclined Lorentz force: an approach to entropy optimization. *J. Therm. Anal. Calorim.* (2020). <https://doi.org/10.1007/s10973-020-09751-3>
39. M. Khan, A. Shahid, M. El Shafey, T. Salahuddin, F. Khan, Predicting entropy generation in flow of non-Newtonian flow due to a stretching sheet with chemically reactive species. *Comput. Methods Programs Biomed.* (2020). <https://doi.org/10.1016/j.cmpb.2020.105318>
40. Y.X. Li, M.I. Khan, R.J.P. Gowda, A. Ali, S. Farooq, Y.M. Chu, S.U. Khan, Dynamics of aluminum oxide and copper hybrid nanofluid in nonlinear mixed Marangoni convective flow with entropy generation: Applications to renewable energy. *Chinese. J. Phys.* **73**, 275–287 (2021). <https://doi.org/10.1016/j.cjph.2021.06.004>
41. S. Ahmad, S. Nadeem, N. Muhammad, M.N. Khan, Cattaneo-Christov heat flux model for stagnation point flow of micropolar nanofluid toward a nonlinear stretching surface with slip effects. *J. Therm. Anal. Calorim.* **143**, 1187–1199 (2021). <https://doi.org/10.1007/s10973-020-09504-2>

Springer Nature or its licensor (e.g. a society or other partner) holds exclusive rights to this article under a publishing agreement with the author(s) or other rightsholder(s); author self-archiving of the accepted manuscript version of this article is solely governed by the terms of such publishing agreement and applicable law.